Separation and Purification Technology 212 (2019) 355–367

Contents lists available at ScienceDirect

Separation and Purification Technology

journal homepage: www.elsevier.com/locate/seppur

Filtration of the catalyst suspension in hydrogenated oil through the woven cloth: Mathematical model of the process accounting for dynamics of the cake growth and filter pore blockage

N.V. Vernikovskaya*, V.A. Chumachenko, A.V. Romanenko, N.M. Dobrynkin

Boreskov Institute of Catalysis SB RAS, Pr. Ak. Lavrentieva 5, Novosibirsk 630090, Russia

ARTICLE INFO

Keywords:
Depth filtration
Cake filtration
Catalyst suspension
Particle size distribution
Mathematical modeling

ABSTRACT

Catalytic hydrogenation of the plant oils includes a filtration stage in which the solid catalyst must be separated from its suspension in the melted hydrogenation products. For effective separation of the catalyst, a proper selection of the filter cloth and filtration conditions is necessary.

The subject of this study is filtration of finely dispersed carbon material *Sibunit* through a porous woven filtering cloth in circulation mode. *Sibunit* is the carrier for Pd catalysts that are regarded as prospective for hydrogenation of vegetable oils; the carbon-based catalysts can be reused and can therefore be more economical than conventional nickel catalysts. To reliably predict the efficiency and duration of filtration of the catalyst suspended in the hydrogenated products, the mathematical model of the filtration process must adequately describe the complex physical phenomena that occur during the process.

In the article, a one-dimensional mathematical model was developed, which took into account the main physical phenomena of the filtration process, such as percolation of the particles through a porous filter, accumulation of the particles along the filter pores, and a gradual cake growth. Woven fabric contains two types of pores: the pores between the threads and the pores between the fibers. Model assumes that polydisperse particles can both penetrate through the filter cloth and accumulate inside the tissue and on its outer surface. It is assumed that the hydraulic resistance of the cake increases due to the growth of its height only, and the hydraulic resistance of the filter cloth increases due to particles trapped in the pores.

Numerical analysis of the model was carried out in the range of parameters typical for industrial conditions. It has been found that the process efficiency, which was defined as the minimum time required filtering a certain amount of hydrogenated oil to the maximum degree of catalyst purification, depends mainly on the time taken to form a cake layer of sufficient height. Higher efficiency of the filtration process is favored by the higher filter porosity, the greater thread diameter, and the smaller pore size between the fibers. In contrast to the thin pores formed by the fibers, the large pores between threads allow more particles to pass through the filter; therefore, for practical use it is necessary to adjust the filter cloth porous structure with the particles size distribution.

The model was verified by comparing the predicted results with experimental data.

1. Introduction

Catalytic hydrogenation of vegetable oils that are liquid at ambient temperature is aimed at improving their oxidative stability during storage and processing. The composition of fatty acids and organoleptic properties of hydrogenated oils depend on the process conditions and the catalyst employed. Conventional hydrogenation technologies are based on various Ni-kieselguhr catalysts. After hydrogenation in the slurry reactor, the catalyst must be carefully separated from the melted products on filters, to fit the mandatory regulations on the content of heavy metals in foods [1–3]. Alternative catalysts such as Pt and Pd supported on silica, carbons etc. are much less harmful, and they exhibit higher activity and lower trans-isomerizing ability but are more expensive [4–6]. Due to the evident economic reasons, such catalysts should be reused in a cyclic manner, by periodic separating them from the products and recycling to the process. Considering that the nature, properties and forms of the carriers for Pd/Pt catalysts differ significantly from those for Ni catalysts, studies on the proper filtration of the catalysts containing noble metals are the key technological issues.

Particles of catalyst may vary in size from the very fine fractures to

* Corresponding author.
E-mail address: vernik@catalysis.ru (N.V. Vernikovskaya).

https://doi.org/10.1016/j.seppur.2018.11.007
Received 14 June 2018; Received in revised form 24 October 2018; Accepted 2 November 2018
Available online 03 November 2018

Nomenclatures

$b_k = -0.5\cdot\ln(1-\varepsilon_k) - 0.52 + 0.64\cdot(1-\varepsilon_k) + 1.43\cdot\varepsilon_k\cdot Kn_k$	coefficient in Eqs. (17)
	cunningham factor
C_k^i	concentration of the particles of *i-th* size in suspension inside the *k-th* pore of the filter cloth, kg/m^3
C_k^{all}	concentration of the particles of all sizes, accumulated in the *k-th* pore of the filter cloth, kg·m^{-3};
C^{iin}	concentration of the particles of *i-th* size in the flow up to the filter cloth, kg·m^{-3}
C^{idep}	concentration of deposited particles on the surface of the filter due to inertial impactionion and if the particle size is larger than pores diameter, kg·m^{-3}
C^{in}	concentration of dry particles of all sizes in the flow up to the filter cloth, kg·m^{-3}
d	diameter, μm
d_1, d_2	diameter of pores between the separate fibers (1st type pores) and pores between the threads, or filaments (2nd type pores)
d_{f1}, d_{f2}	diameter of the separate fibers and the threads, or filaments
J	number of grid points in spatial discretization
G	mass of filtered suspension, kg
H_{cake}	height of cake, m
H^*_{cake}	height of cake, when particles cannot penetrate into the filter medium but deposit on the surface, m
K	coefficients in Eqs. (12),(13)
K_B	Boltzmann constant
$Kn_k = d_{liquid}\cdot(\sqrt{1-\varepsilon_k})/(\sqrt{\varepsilon_k}\cdot d_k)$	Knudsen number
L	thickness of filter cloth, m
m	mass of deposited particles on the surface of the filter, kg
m^{in}	mass of particles entered the filter, kg
m^{out}	mass of particles left the filter, kg
$\bar{m}$	mass of particles remained in liquid inside the pores of the filter cloth, kg
$\bar{\bar{m}}$	mass of particles captured in the pores of the filter cloth, kg
n	ratio of the weight of dry catalyst particles to wet ones
N_k	number of particles sizes in the *k-th* pore of the filter cloth
ΔP	pressure, mPa
$Q_k^i = d_p^i/d_{fk}$ $Pe_k^i = u\cdot d_{fk}/(10^5\cdot C\cdot K_B\cdot T/(3\cdot\pi\cdot\mu\cdot d_p^i))$	
R	hydraulic resistance, m^{-1}
S	outer surface area of the filter, m^2
$St_k^i = C\cdot\rho_{solid}/(1-\varepsilon_c)\cdot(d_p^i)^2\cdot u/(9\cdot\mu\cdot d_{fk})$	Stokes number
T	temperature, °C
t	time, s
t_n	TIME necessary to passing of suspension batch through the filter, min
$t_{H^*_{cake}}$	time of reaching cake height equal to H^*_{cake}
Δt	time increment, s
$u = \frac{1}{S}\left(\frac{dV_{Filtrate}}{dt}\right)$	filtration rate, m·s^{-1}
$V_{Filtrate}$	volume of filtrate collected, m^3
V_{cake}	volume of cake, m^3
x	axial coordinate along the filter cloth, m
Δx	Axial coordinate along the filter cloth, m

Greek letters

$\chi(t)$	degree of suspension purification from the catalyst for process time t
ε	porosity
φ_k	depth of particle penetration into the filter medium, m^{-1}
η_k^i	overall efficiency of filtration due to particles of i-th size capturing in suspension inside the k-th pore of the filter cloth
$\eta_{k\,imp}^i$	efficiency of filtration due to inertial impact
$\eta_{k\,int}^i$	efficiency of filtration due to interception
$\eta_{k\,dif}^i$	efficiency of filtration due to particles diffusion
$\eta_{k\,int+dif}^i$	combined efficiency of filtration due to particles interception and diffusion
μ	viscosity, kg m^{-1} s^{-1}
ρ	density, kg m^{-3}

Subscripts

c	cake
ev	average
F	filter cloth
f	fiber
in	inlet
k	*k-th* pore of the filter cloth
liquid	liquid phase
out	outlet
p	particle
solid	solid phase

Superscripts

0	initial value
i	*i-th* size of the particles

the coarse ones. If the particles are larger than the filter cloth pores or comparable in size, they deposit on its surface. This process is called *cake filtration*. If the particles are smaller than the filter cloth pores, they percolate through its medium or accumulate inside it which causes the pores blockage. This process is called *depth filtration*. As soon as the cake height grows large, the particles do not penetrate into the filter. Even small amounts of the fines and the middle-size particles captured inside the filter medium can significantly increase its hydraulic resistance and reduce filtration rate, especially at the beginning of filtration. Usually, theoretical and experimental studies of the filtration process similar to this are limited to accounting for only cake filtration [7–16], or only depth filtration [17,18]. As a rule, the depth filtration is not taken into account in the mathematical models, only the hydraulic resistance of the clean, i.e. having no captured particles filter medium is considered. In this article, the study is focused on formulating a mathematical model that describes the filtration of catalyst suspension process, taking into account both the cake growth and depth filtration. In addition, the particle size distribution is considered in depth filtration. It is assumed that the porosity and pore diameter of the cake do not change and the hydraulic resistance increases due to the growth of the height of the cake only. At depth filtration, when calculating the hydraulic resistance, the decrease in porosity and pore diameter due to trapped particles are taken into account. The main purpose of this work is to study the dynamics of filtration of a catalyst suspension with a known particle size distribution; namely, the dynamics of particles percolation through the filter pores and their accumulation along the filter, as well as the dynamics of the cake growth. Experimental studies, which were carried out under conditions close to industrial, confirmed the validity of the theoretical premises of the model.

The following problems have been investigated and solved in the work:

1. Development of the unsteady-state mathematical model with distributed parameters. Algorithm, numerical code and mathematical

model validity were verified by comparison of the modeling results with experimental data.
2. Assessment of the influence of particle size distributions, porous structure of the filter medium and concentration of the particles in suspension on the filter operation. The filtration through the filter being initially clean and through the filter after several cycles of the particles discharge was studied.
3. Separation of the dispersed mesoporous carbon material *Sibunit* from hydrogenated oils using a commercial woven filtering fabric was studied experimentally on a lab-scale setup.

2. Theoretical formulation of the catalyst filtration problem

In the technologies of the fats hydrogenation in slurry reactors, cartridge-type filters of periodic action are used downstream the reactor unit. On the filtering surface, an alluvial layer of the filtered catalyst particles is gradually formed. This top layer has larger filter channels in comparison with the pores of the filter cloth, which directly contributes to the uniform deposition of the sludge onto the filter surface and improves the filtration efficiency.

The process of filtration is shown schematically in Fig. 1. The porous structure of the filter consists of pores between the separate fibers (1st type pores) and pores between the threads, or filaments (2nd type pores); the total pore volume is the sum of its constituent volumes. It is assumed that the catalyst particles size distribution is known.

Depending on the size of the particles entering the pores, they can either be deposited on the walls of the pores, or pass through the pores and leave the filter cloth along with the convective fluid flow. The following mechanisms for trapping particles in pores are taken into account: inertial collision, interception, diffusion, interaction between interception and diffusion [19–26]. The concentration of catalyst particles suspended in liquid inside the pores of the filter cloth (liquid phase) varies along the length of the pore and changes in time. The mass of catalyst particles trapped on the pore walls (solid phase) is also changes. With increasing the mass of particles trapped inside the pores, the pore diameter and porosity decrease, while the effective diameter of the fiber (thread) increases. As a result, the pressure drop of the filter cloth increases, this leads to a decrease in the filtration rate.

If the catalyst particles that are fed with the liquid flow to the surface of the filter cloth are greater than the pore size, they cannot enter the pores and are deposited on the surface of the filter. The catalyst particles that are deposited on the surface of the filter also cannot enter the pores due to inertial collision, even if their size is less than the pore diameter.

Catalyst particles accumulated on the outer surface of the filter cloth form a cake layer; its thickness is growing gradually. The height of the cake layer can be influenced by various factors; in particular, the concentration of solids in the suspension. The particles that were trapped in the pores, or were settled in the pores as the suspension, or penetrated through the filter cloth do not contribute to the formation of the cake. The growth of the cake's height also leads to an increase in hydraulic resistance and a decrease in the rate of filtration.

2.1. Mathematical model

To describe the process of filtering a suspension of solid particles through a porous cloth filter, a one dimensional mathematical model was developed. The model takes into account the main features of the system, as follows:

- Unsteady-state behavior;
- Heterogeneity;
- Convective mass transfer of particles in liquid along the filter depth;
- Penetration of particles through the filter;
- Accumulation of particles inside the filter pores due to inertial collision, particle interception, diffusion and their combined influence;
- Deposition of coarse particles and particles due to inertial collision on the outer filter surface;
- Two types of pores in filter cloth;
- Particles size distribution.

The model also assumes that: (i) porosity, pore diameter and other structural properties of the cake layer do not change in time; (ii) after the cake's height has reached a critical value of H^{*}_{cake}, the particles can

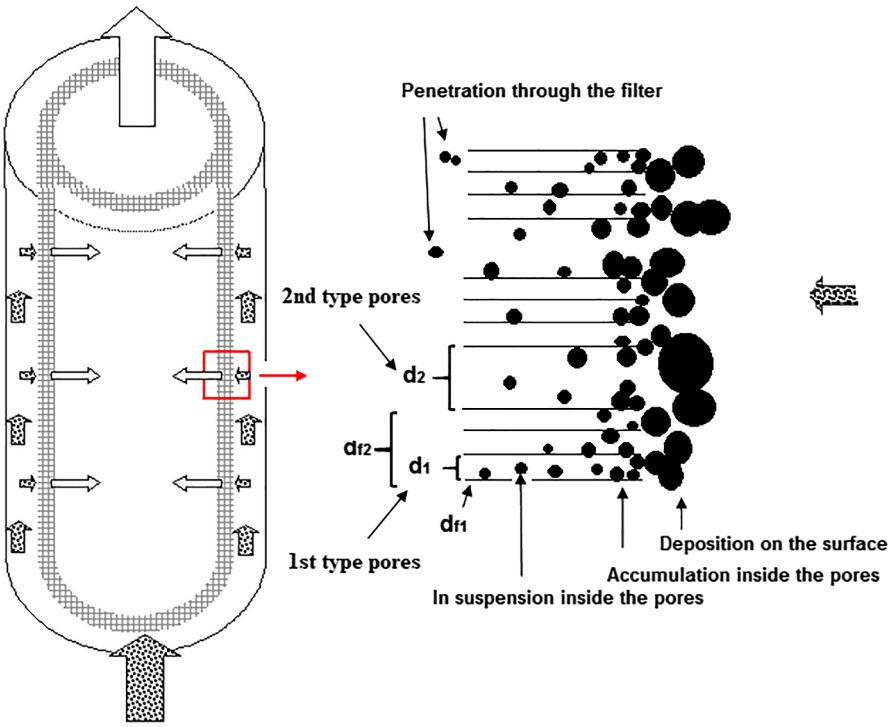

Fig. 1. A scheme of the filtration process.

no longer penetrate the filter, but settle on its outer surface.

2.1.1. Equations for the filter cloth

Model equations of material balance for filter cloth are written in relation to:

- The concentration of the particles of *i-th* size in the suspension inside the *k-th* pore of the filter cloth:

$$\varepsilon_k \frac{\partial C_k^i}{\partial t} + \frac{1}{S}\left(\frac{\partial V_{Filtrate}}{\partial t}\right)\frac{\partial C_k^i}{\partial x} = -C_k^i \cdot \eta_k^i \cdot \varphi_k \cdot \frac{1}{S}\left(\frac{\partial V_{Filtrate}}{\partial t}\right),\ i = 1, \bar{N}_k,\ k = 1, 2 \quad (1)$$

The first term of Eq. (1) describes the dynamic variation of the concentration of *i-th* size particles in liquid inside the *k-th* pore of the filter cloth. The second term corresponds to convective mass transfer along the depth of the filter cloth. Third term describes decreasing of the particles concentration due to their capturing in the *k-th* pore of the filter cloth.

- The concentration of the particles of all sizes, accumulated in the *k-th* pore of the filter cloth:

$$\frac{\partial C_k^{all}}{\partial t} = \varphi_k \cdot \frac{1}{S}\left(\frac{\partial V_{Filtrate}}{\partial t}\right) \cdot \sum_{i=1}^{N_k} C_k^i \cdot \eta_k^i,\ k = 1, 2 \quad (2)$$

Eq. (2) describes the dynamic variation in mass content of all particles in the *k*-th pore due to their capturing. C_k^{all} depends also on the coordinate along the thickness of the filter cloth (x).

Individual Eq. (1) for concentrations of *i*-th size particles were given in [25,26] accounting for the trapping in porous filters the soot particles from diesel engine exhaust. In contrast to that case, we assume here that the particles are suspended in liquid, the pores are of different sizes, and the filtration rate $\frac{1}{S}\left(\frac{dV_{Filtrate}}{dt}\right)$ is changing in time.

The collection efficiency (η_k^i) of particles of *i*-th size in a *k*-th pore depends on the particles size, pore diameter, porosity and fiber diameter. The depth of particle penetration into the filter medium (φ_k) depends on the porosity and fiber diameter. The pore diameter, porosity and fiber diameter can vary along the filter thickness due to their dependence on the concentration of the particles, accumulated in *k*-th pore of the filter cloth (C_k^{all}) which is varying along the filter thickness as well. Formulae for determination of (η_k^i) and (φ_k), as well as for pore diameter, porosity and fiber diameter are given in Section 2.1.5.

2.1.2. Equations for the cake

The equations of the model that describe the cake height growth are given below. The cake height is determined as:

$$H_{cake} = \frac{V_{cake}}{S} \quad (3)$$

To calculate the volume of particles that settle on the filter surface without penetration inside, the following expression was proposed in [27]:

$$V_{cake} = \left(\frac{m}{\rho_{solid}} + \frac{m \cdot (n-1))}{\rho_{liquid}}\right) \quad (4)$$

Here m is the mass of the particles entrapped on the filter cloth surface; it is equal to the total mass of the particles entered the filter [27].

In the filtration process we study here the deposition of particles in the pores of the filter cloth is taken into account. Therefore, from the mass balance, the quantity (m) will be equal to the mass of particles entering the filter per unit time (m^{in}), except for the mass of particles that passed through the filter (m^{out}), remained in the liquid phase inside the pores ($\bar{m}$) and captured on the walls of pores ($\bar{\bar{m}}$), per the same unit time:

$$m = m^{in} - m^{out} - \bar{m} - \bar{\bar{m}} \quad (5)$$

Here,

$$m^{in} = \sum_{i=1}^{N_k} C^{i\,in} \cdot \left(\frac{dV_{Filtrate}}{dt}\right) \cdot \Delta t \quad (6)$$

$$m^{out} = \sum_{k=1}^{2} \sum_{i=1}^{N_k} C_k^{iout} \cdot \left(\frac{dV_{Filtrate}}{dt}\right) \cdot \Delta t \quad (7)$$

$$\bar{m} = \sum_{k=1}^{2} \varepsilon_k \int_0^L \sum_{i=1}^{N_k} C_k^i \cdot dx \cdot S \quad (8)$$

$$\bar{\bar{m}} = \sum_{k=1}^{2} \int_0^L C_k^{all} \cdot dx \cdot S \quad (9)$$

Thus, the height of the cake at each time may be expressed as:

$$H_{cake}(t) = \frac{m^{in} - m^{out} - \bar{m} - \bar{\bar{m}}}{S} \cdot \left(\frac{1}{\rho_{solid}} + \frac{(n-1)}{\rho_{liquid}}\right) \quad (10)$$

2.1.3. Equation to calculate the rate of filtration

When the suspension is filtering, the total hydraulic resistance of the filter is composed of the resistances of the cake layer (R_{cake}) and of the filter cloth (R_F). In assumption that the cake layer and the filter cloth are homogeneous porous media, the Kozeny – Carman equation [27,28] may be used to describe their individual contributions to the total resistance:

$$\Delta P = (R_{cake} + R_F) \cdot \mu \cdot \frac{1}{S}\left(\frac{dV_{Filtrate}}{dt}\right) \quad (11)$$

Here,

$$R_{cake} = K_c \cdot \frac{(1-\varepsilon_c)^2}{\varepsilon_c^3 \cdot d_c^2} \cdot H_{cake} \quad (12)$$

$$R_F = K_F \cdot \int_0^L \frac{(1-\varepsilon_{av})^2}{\varepsilon_{av}^3 \cdot d_{av}^2} \cdot dx \quad (13)$$

We assume here that the physical properties of the cake do not change in time, so the hydraulic resistance of the cake layer may increase only due to the H_{cake} growth. As the particles are trapping in the pores, the porosity of the filter and the pore diameter decrease, which leads to an increase in the hydraulic resistance of the filter. The filter material has two types of pores, which occupy different volumes: pores of the first type have porosity ε_1 and pore size d_1, pores of the second type ε_2 and d_2, respectively; therefore, in formula (13) average pore size, d_{av} and porosity, ε_{av} should be determined proportionally to their fraction in the filter. The porosity ε_k and pore size d_k for pores of each type k strongly depend on the amount of particles captured inside the filter cloth and they are determined by Eqs. (18), (19) (See Section 2.1.6). Therefore, the hydraulic resistance of the filter cloth changes as the filter cloth is filled.

It follows from the Eq. (14) that the filtration rate depends on the pressure drop across the filter medium with the cake upon it, the suspension's viscosity, the cake's height, and on the total hydraulic resistance of the cake and the filter medium:

$$\frac{1}{S}\left(\frac{dV_{Filtrate}}{dt}\right) = \frac{\Delta P}{\mu\left(K_c \cdot \frac{(1-\varepsilon_c)^2}{\varepsilon_c^3 \cdot d_c^2} \cdot H_{cake} + K_F \cdot \int_0^L \frac{(1-\varepsilon_{av})^2}{\varepsilon_{av}^3 \cdot d_{av}^2} \cdot dx\right)} \quad (14)$$

2.1.4. Initial and boundary conditions

To solve differential Eqs. (1), (2) and (14), the following initial and boundary conditions should be added:

$$t = 0:\ V_{Filtrate} = 0;\ \frac{1}{S}\left(\frac{\partial V_{Filtrate}}{\partial t}\right) = u^0;\ C_k^{all} = 0;\ C_k^i = 0;$$
$$i = 1, \bar{N}_k,\ k = 1, 2$$
$$x = 0:\ C_k^i = C^{inn} - C^{idep};\ i = 1, \bar{N}_k,\ k = 1, 2 \quad (15)$$

Here $C^{i\,dep}$ are concentrations of particles deposited on the filter surface due to inertial collision and that of particles whose size was larger than the pore diameter.

2.1.5. Efficiency of particles trapping in pores of filter cloth

The ability to capture the particles is the most important characteristics of the filter's efficiency; it is governed by several factors, such as: (a) inertial collision while the particles are colliding with the fibers; (b) interception of the particles while they are passing near the fibers; (c) diffusion of particles; and (d) joint influence of the particles interception and diffusion.

According to [19–26], the overall filtration efficiency may be written as:

$$\eta_k^i = \eta_{k\,imp}^i + \eta_{k\,int}^i + \eta_{k\,dif}^i + \eta_{k\,int+dif}^i;\ i = 1, \bar{N}_k,\ k = 1, 2 \tag{16}$$

Here, the empirical correlations for specific efficiencies are presented as:

$$\begin{aligned}
\eta_{k\,imp}^i &= 3.2\cdot 10^3 \cdot e^{10.5\cdot St_k^i} \\
\eta_{k\,int}^i &= 1/(2\cdot b_k)\cdot \\
&(1/(1+Q_k^i) - (1+Q_k^i) + 2\cdot(1+Q_k^i)\cdot\ln(1+Q_k^i) \\
&+ 2.86\cdot Kn_k\cdot(2+Q_k^i)/(1+Q_k^i)) \\
\eta_{k\,dif}^i &= (2.7/Pe)\cdot(1+0.39\cdot(b_k)^{-1/3}\cdot Pe^{1/3}\cdot Kn_k) \\
\eta_{k\,int+dif}^i &= 1.24\cdot(Q_k^i)^{2/3}/((b_k)^{1/2}\cdot Pe^{1/2});\ i = 1, \bar{N}_k,\ k = 1, 2
\end{aligned} \tag{17}$$

Note that the values of $\eta_{k\,imp}^i$, $\eta_{k\,int}^i$, $\eta_{k\,dif}^i$, $\eta_{k\,int+dif}^i$ are varying along the height of the filter cloth (coordinate x) and with time, because they depend on changing values of the filter porosity, pore sizes and fiber diameters. As the particles are trapping inside the pores, the porosity and pore sizes decrease, and fiber diameters increase.

2.1.6. Parameters of the filter medium

The effective values of the filter parameters such as porosity, pore sizes and fiber diameters strongly depend on the amount of particles captured inside the filter cloth, and therefore these parameters vary along the filter cloth thickness (coordinate x). Parameters could be determined from the expressions (18), (19), (20) as follows:

$$\varepsilon_k = \varepsilon_k^0 \cdot \frac{\rho_{solid} - n\cdot C_k^{all}/\varepsilon_k^0}{\rho_{solid}},\ k = 1, 2 \tag{18}$$

$$d_k = d_k^0 \cdot \sqrt{\frac{\rho_{solid} - n\cdot C_k^{all}/\varepsilon_k^0}{\rho_{solid}}},\ k = 1, 2 \tag{19}$$

$$d_{fk} = d_{fk}^0 \cdot \sqrt{1 + \frac{2\cdot C_k^{all}/\varepsilon_k^0}{\rho_{solid}\cdot(1-\varepsilon_k^0)}},\ k = 1, 2 \tag{20}$$

The depth of particle penetration into the filter cloth depends on the initial filter porosity and on the fiber or thread diameter; it depends also on the current value of the fiber or thread diameter:

$$\varphi_k = \frac{4\cdot(1-\varepsilon_k^0)}{\pi\cdot(d_{fk}^0)^2}\cdot d_{fk},\ k = 1, 2 \tag{21}$$

2.2. Method for solving the equations of the model

To discretize the set of partial differential Eq. (1) into the large set of ordinary differential equations (ODE) with time as an independent variable, the method of lines have been applied. Eq. (2) for each space grid point of the filter medium ($j = 0, 1,\ldots,J$) was included into this set of differential equations of the 1st order. Initial and boundary conditions (15) and Eqs. (16)–(21) were also taken into account. For solving this set, a running scheme was used: the corresponding subset of ODE's for each space grid point j was solved from t to $t + \Delta t$ in series in the streamwise direction (successively for $j = 0, 1,\ldots,J$). A special case of the 2nd order Rosenbrock method and an automatic selection of the internal integration step were employed for solving the ODE set at each space-grid point j from t to $t + \Delta t$ [25,29,30]. The required current values from $(j-1)$-th point were obtained by means of interpolation procedure. Ordinary differential Eq. (14) was solved analytically from t to $t + \Delta t$, taking into account Eqs. (5)–(10).

2.3. Determination of the model parameters

The values of the model parameters are listed in Table 2; some of them have been estimated from the experimental results after procedures presented below.

Filtration rate. The initial filtration rate was determined as:

$$u^0 = \frac{G}{t_n\cdot\rho_{liquid}\cdot S} \tag{22}$$

Under the experimental setup conditions (see Chapter 3), G = 40 kg, t_n = 54 s, hence, $u^0 = 0.01\ m/s$.

Filter cloth pore sizing. The diameter of the 1st type pores, d_1^0, was taken equal to the diameter of the separate fiber (20 μm). The diameter of the 2nd type of pores, d_2^0 = 42 μm, was estimated from the SEM-image (Fig. 2) and proved experimentally. Inspecting the particles size distribution after filter detected no particles larger than 42 μm in diameter in the post-filtered suspension.

The diameter of the thread (Fig. 2), d_{f2}^0 = 375 μm, was determined as the arithmetic mean between the thread sizes at its narrowest and widest fragments.

Other parameters are determined in Appendix.

3. Experimental

3.1. Experimental setup

A general view of the lab-scale setup is shown in Fig. 3. The setup reproduces in scale 1:250 the element of industrial cartridge-type filter. It includes a thermally insulated filter, a tank filled with a solid suspension in melted fat, a circulating pump, a mixer, a heater and a transparent glass tube for monitoring the filtration progress. The height and diameter of the filter are 0.22 and 0.087 m, respectively, the filtration surface is 0.06 m^2.

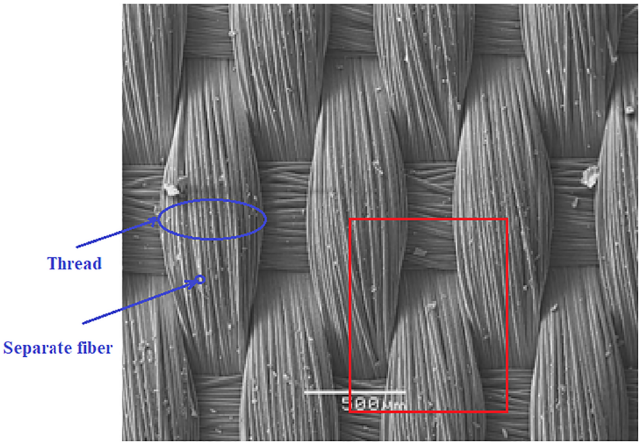

Fig. 2. SEM-image of the commercial woven filter material. The fragment inside red square was used to estimate the porosity formed by the second type pores, ε_2^0. (For interpretation of the references to colour in this figure legend, the reader is referred to the web version of this article.)

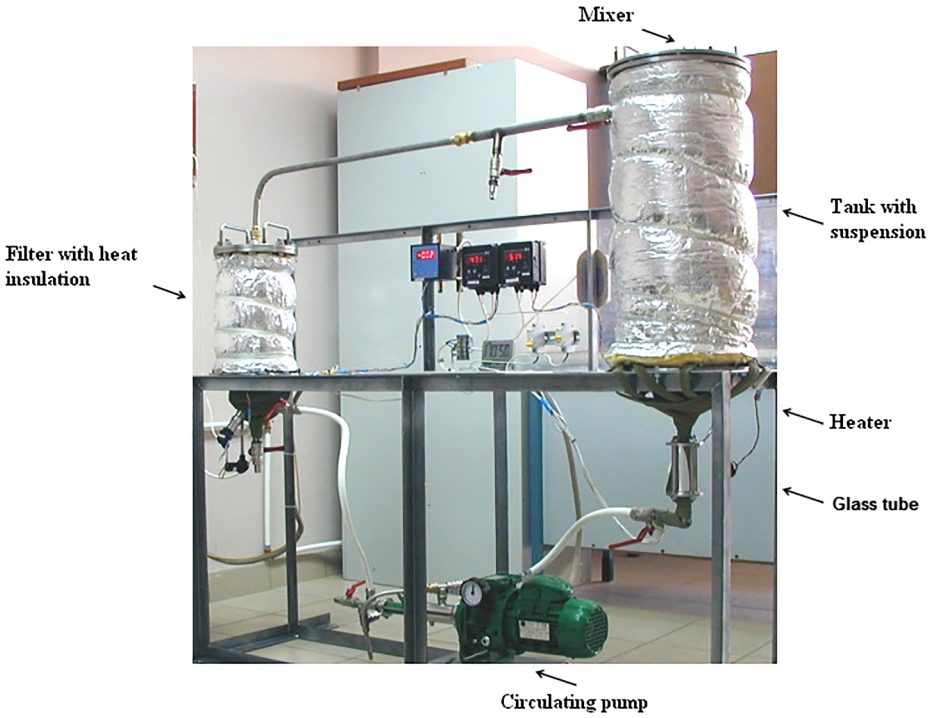

Fig. 3. A general view of the experimental setup.

3.2. Filtering material

In the filter, a commercial synthetic woven filtering fabric was stretched over a rigid metal frame. A SEM image of this material obtained using JSM-6460 LV (*Jeol*) device is presented in Fig. 2. An individual fiber was ~ 20 μm in diameter, a thread twisted from multiple fibers was 250–500 μm thick.

3.3. Oils mixture

For experimental studies, the product of hydrogenation of the fats blend consisted of palm olein, sunflower oil, and palm stearin was used. Melting point was 40 °C, viscosity and density at 80 °C were 20 mPa·s and 855 kg/m^3, respectively.

3.4. Solid material

Mesoporous carbon material *Sibunit* is regarded as prospective support for Pd catalyst in hydrogenation process [6]. A dust-free sample of this material was used in experiments, the morphology of *Sibunit* particles is shown in Fig. 4. The major physical characteristics of this support are presented in Table 1. The BET specific surface area of the sample was determined using the ASAP-2400 (*Micromeritics*) automatic volumetric device; the procedure was based on the adsorption of N_2 at 77 K. The particle size distribution analysis was performed on the test sieve shaker *HAVER EML 200 digital plus T*.

3.5. Experimental procedure and results

Initially, a batch of 20 kg fats blend was loaded and melted in the tank at 75 °C, then 40 g solids were added, and suspension was mixed during 30 min. The mass ratio 1:500 between solid and liquid phases was identical to the concentration of the catalyst loaded in commercial hydrogenating slurry reactors.

Experimental procedure consisted in continuous recycle-mode filtering of the suspension of particles in a melted fat medium through a filter cloth. The suspension was fed up from the filter bottom. Temperature and the pressure drop between two sections of the filter were kept at 75 °C and 0.25 MPa, respectively. Due to the pressure drop between the inner and outer chambers of the filter, clean oil percolated through the filter cloth. Particles penetrated through the filter or accumulated both inside it and on its surface, depending on the particle size. The pressure drop was kept constant by controlling the rate of the suspension feeding via adjustment the screw-type pump and the degree of the bypass opening.

Another portion of 40 g of solids was added in 50 min to the tank to give the necessary (identical to that in the commercial filter) quantity ratio of the solid phase and the filter surface. Then the solids were added in every 50 min. When the pressure drop between two sections exceeded 0.25 MPa the filtration process was stopped. The filter was cleaned from the solids by blowing the compressed air 0.45 MPa, then the process was twice repeated.

Time duration which is necessary for complete removal of the given solids volume from suspension (t_n) is the main parameter to be determined. While the filtration rate decreases due to the particles

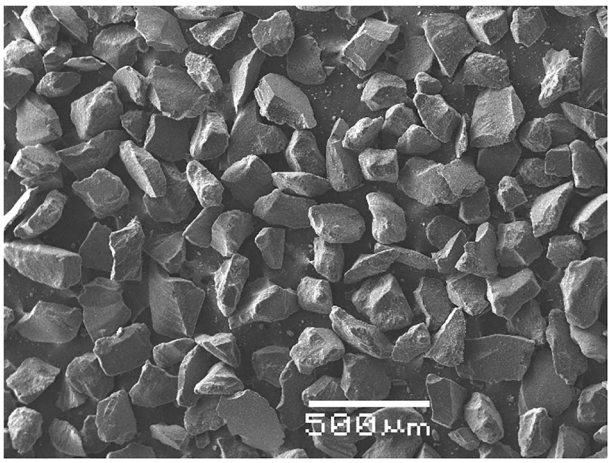

Fig. 4. SEM-image of the dust-free mesoporous carbon material *Sibunit*.

Table 1
Specifications of *Sibunit* carbon support.

Parameter	Value
Specific surface area (S_{BET}), $m^2 \cdot g^{-1}$	304
Bulk density (as dry powder), $kg \cdot m^3$	463
Size distribution (as mass fractions), wt. %	
< 50 μm	1.8
50–100 μm	1.9
100–200 μm	94.1
> 200 μm	2.2

deposition in the pores and on the filter surface, t_n gradually increases in time. Assuming that 40 kg suspension batch with added 80 g of catalyst particles is identical to 0.2 wt% catalyst loading in the industrial slurry reactor, the t_n value can be calculated as:

$$t_n = \frac{1}{S} \cdot \frac{40\,kg}{\rho_{liquid} \cdot \frac{1}{S} \cdot \frac{dV_{Filtrate}}{dt}} \tag{23}$$

The values of t_n were estimated experimentally in the course of three consecutive filtration cycles; time durations versus time elapsed are plotted in Fig. 5. Each cycle consisted of a series of solids loading without intermediate filter cleaning and continued until the liquid phase becomes completely transparent; then the filter was cleaned from the trapped particles. In Fig. 5, squares correspond to filtration through initially clean filter, circles – through the filter after the 1st particles discharge, triangles – after the 2nd particles discharge. In the chapter to follow, experimental data will be compared with theoretical predictions obtained by the process modeling.

4. Results and discussion

Mathematical model of the filtration allowed to analyze the role of various process parameters such as the catalyst particles size distribution, the porous structure of the filter medium, concentration of the catalyst particles in suspension. Their influence on the filtration rate and the filtration time, cake's height, hydraulic resistance of the filter cloth and cake was studied in a wide range of parameters.

4.1. Filtration of suspensions when taking into account particles size distribution

The influence of the particle size on the filtration is simulated. Particles size distribution in the bulk flow may differ from that at the pore inlet. Coarse particles whose size is larger than the pore size cannot penetrate the pores and are deposited on the outer surface of the filter cloth. The particles not larger than 20 and 42 μm in size can only enter the 20 and 42 μm pores of the 1st and the 2nd types, respectively. The particles whose size is smaller than the pore size can be settled on the filter surface as well, due to the mechanism of inertial impact, at efficiency $\eta^i_{k\,imp}$. However, as the initial filtration rate is not high, $u^0 = 0.01$ m/s, only minor fraction of all particles (estimated as ≤0.1%) can be deposited on the surface due to the inertial impact. In general, the particles can either percolate the pores or deposit on the outer surface to form the cake layer.

When entering the pores of the filter cloth, the particles of any size are captured on the pore walls; the capturing of larger particles is more effective than the smaller ones.

In the Fig. 6, the calculated profiles of parameters along the 1st type pores are depicted. Fig. 6a shows the profiles of relative particle concentration in the liquid inside the pores C_1^i; particles 5 μm in size penetrate the filter deeper than particles of 7 μm or more. This is due to the fact that the capturing efficiency and the role of particles interception and diffusion decreases with decreasing the particles size (Eq. (17)); therefore, the total efficiency of the particle capturing in the pore surface also decreases. Fig. 6b shows concentration profiles of captured particles C_1^{all} along the filter depth at various times from the filtration onset. At the beginning, particles are trapped nearby the filter surface, and then concentration gradually increases, which correlates to the reduction of the filter porosity ε_1 (Fig. 6c) and the pores diameter d_1 (Fig. 6d). Initially, the profiles of filter porosity and the pores diameter are uniform along the filter depth (shot dashed lines), then decline due to the pore blockage. At the same time, the apparent fiber diameter d_{f1} increases due to the capturing effect (Fig. 6e). The particles are captured in the pores until they are completely filled, or until the cake's height becomes larger than H^*_{cake}. In the case we analyze, the cake height reached H^*_{cake} in 20 min from the process start; the pores were not completely full. It is assumed that the pores are completely filled with particles if their concentration is 90% of the bulk density of dry particles calculated per cubic meters of filter cloth. Hence, the maximum filling with the captured particles corresponds to 140 kg/m^3. Having reached this value, the concentration of captured particles does not increase. All incoming particles deposit on the filter surface, causing an increase in alluvial layer height.

Fig. 7a shows the calculated profiles of relative particle concentration in the liquid inside pores C_2^i along the 2nd type pores. These pores are formed by thick threadsd_{f2} = 375 μm in diameter; that's why their efficiency in particle capturing is lower than that of fine pores due to lower efficiencies factors $\eta^i_{2\,imp}$, $\eta^i_{2\,int}$, $\eta^i_{2\,dif}$, $\eta^i_{2\,int+dif}$ (Eqs. (17)). For this reason, just all the particles can penetrate through the filter cloth from the inlet to the outlet. The specific features of the 2nd type pores filling are similar to ones of the 1st type. Due to the relatively small porosity $\varepsilon_2 = 0.08$, the maximum filling with captured particles in the 2nd type pores is only 3.3 kg/m^3 that is much less than in the 1st type pores. Fig. 7b shows concentration profiles of captured particles C_2^{all} along the filter depth at various times from the filtration onset. At the inlet to the filter cloth, the concentration of captured particles is 0.195 kg/m^3 that is much less than in the 1st type pores. As the filter porosity ε_2 (Fig. 7c) and pores diameter d_2 (Fig. 7d) decrease, the apparent fiber diameter d_{f2} increase (Fig. 7e). The 2nd type pores are filled much more slowly than the 1st type ones, and their complete filling can hardly be achieved. Therefore, particles will be filling pores until the cake layer becomes higher than H^*_{cake} value.

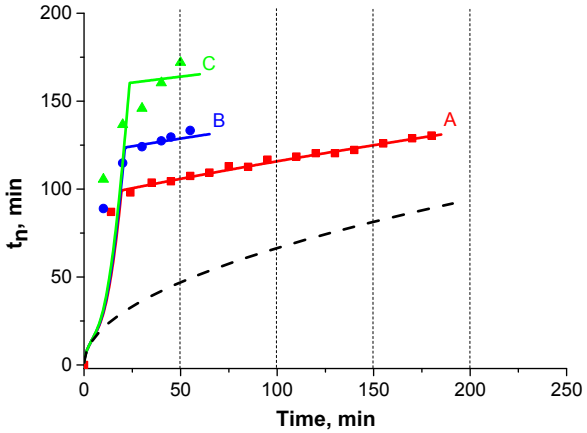

Fig. 5. Experimental and predicted dependences of t_n from the time elapsed. Symbols – experimental data in 3 consecutive cycles of filtration; red squares – 1st cycle, filtration through the filter initially clean; blue circles – 2nd cycle, filtration through the filter after the 1st particles discharge; green triangles – 3rd cycle, filtration through the filter after the 2nd particles discharge. Vertical lines – moments of solids loading. Solid lines – modeling results; for the 1st cycle – line A, particles size distribution is considered (dashed line, only weight-average particles diameter is considered); for the 2nd cycle – line B; for the 3rd cycle – line C. Parameters used for modeling: C^{in} = 1.7 kg/m^3, d_1^0 = 20 μm, $d_{f\,1}^0$ = 20 μm, ε_1^0 = 0.3, d_2^0 = 42 μm, $d_{f\,2}^0$ = 375 μm, ε_2^0 = 0.008. (For interpretation of the references to colour in this figure legend, the reader is referred to the web version of this article.)

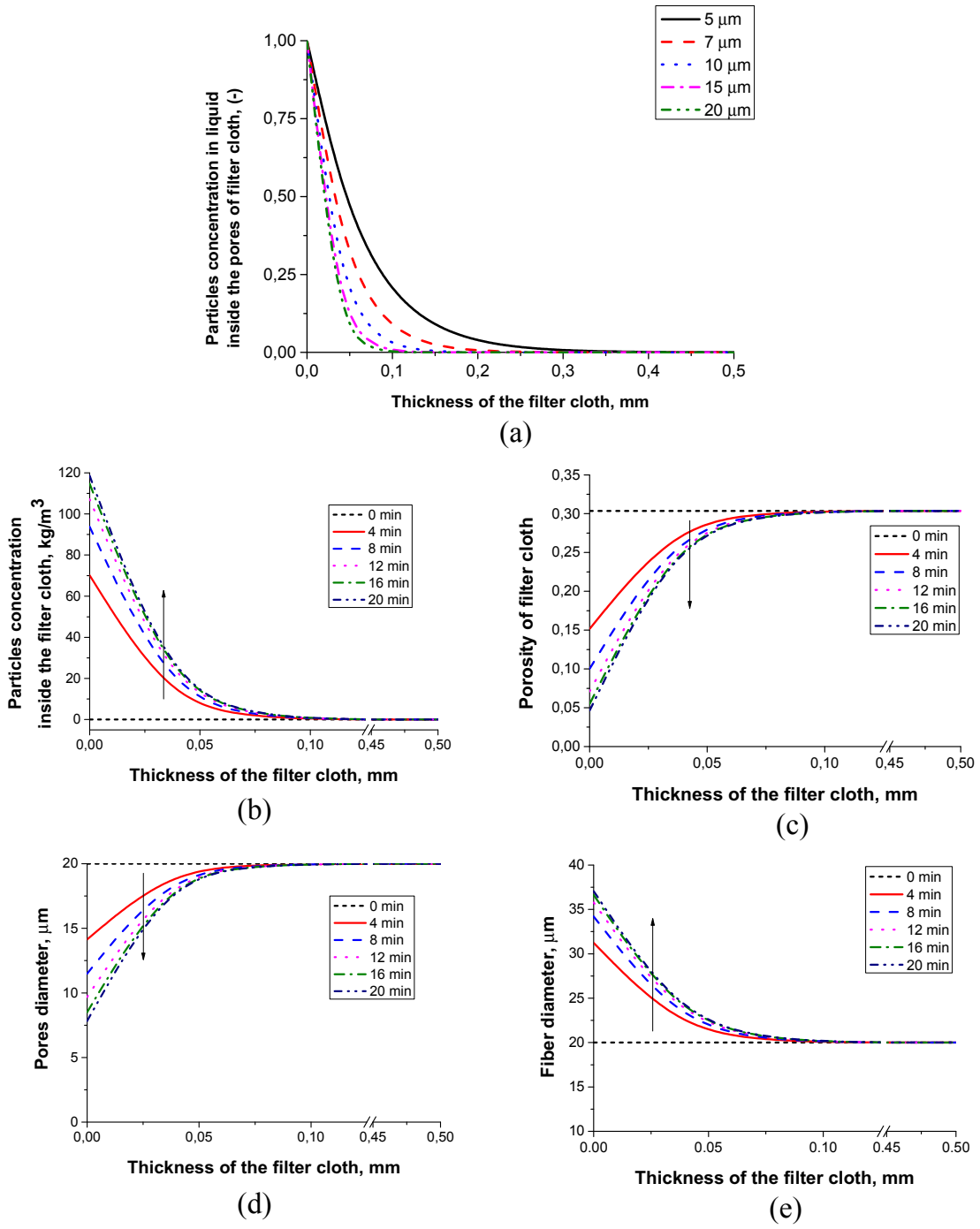

Fig. 6. Simulated profiles of parameters along the filter depth inside the 1st type pores. (a) particles concentration in liquid C_1^i at $t = 6$ s; (b) concentration of captured particles C_1^{all}; (c) porosityε_1; (d) pore diameter d_1; (e) fiber diameter $d_{f\,1}$. Curves refer to various times since the filtration onset. $C^{in} = 1.7$ kg/m^3, $d_1^0 = 20$ µm, $d_{f\,1}^0 = 20$ µm, $\varepsilon_1^0 = 0.3$.

Not all the particles are trapped inside the porous filter and on its surface, some granules penetrate through the filter. Fig. 8 shows the initial, that is, at $t = 6$ s, inlet and outlet concentrations of 5–20 µm particles in the 1st type pores, and inlet and outlet concentrations of 5–42 µm particles in the 2nd type pores. Inside the filter pores of the 1st and 2nd types, there is no particles larger than 20 and 42 µm, respectively, because these particles remain on the surface. Inside the pores of both types, the outlet particle concentration is lower than the inlet one. In the 1st type pores, the outlet concentration of almost all particles is close to zero; however, in the 2nd type pores it's far from zero and only slightly below the inlet concentration, due to a lower capturing efficiency of thick threads that form the 2nd type pores. Note that formation of the cake with pores of 20 µm and height up to three monolayers of the particles prevents larger particles to pass into the 2nd type pores.

On the time diagrams that illustrate the changing of the cake's height (Fig. 9), hydraulic resistance coefficient (Fig. 10a), and the rate of filtration (Fig. 10b), three time intervals which correspond to various rates of the parameter changing can be specified, because these parameters are physically related to each other. The first interval (I) lasts from 0 to 10 min, the second one (II) – from 10 to 20 min, the third one (III) – from 20 min to the process end.

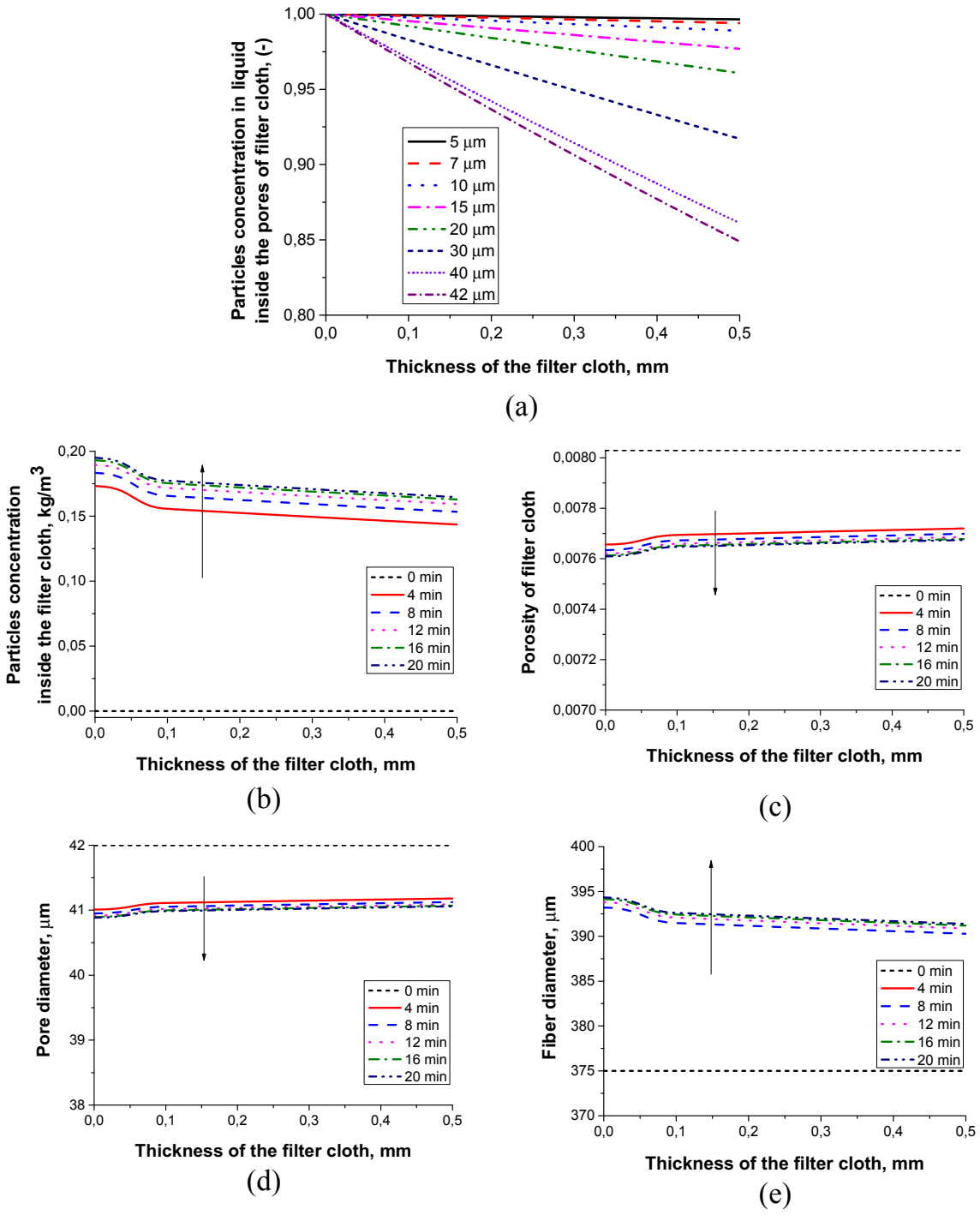

Fig. 7. Simulated profiles of parameters along the filter depth inside the 2nd type pores. (a) particles concentration in liquid C_2^jat $t = 6$ s; (b) concentration of captured particles C_2^{all}; (c) porosity ε_2; (d) pore diameter d_2; (e) fiber diameter $d_{f\,2}$. Curves refer to various times since the filtration onset. $C^{in} = 1.7\,\mathrm{kg/m^3}$, $d_2^0 = 42\,\mu\mathrm{m}$, $d_{f\,2}^0 = 375\,\mu\mathrm{m}$, $\varepsilon_2^0 = 0.008$.

For the time (I), the highest rates of the cake thickening H_{cake} (Fig. 9, solid line) and of the hydraulic resistance R_{cake} (Fig. 10a, dash line) growth were observed, owing to the minor built-up of the captured catalyst particles in the pores (Figs. 6b, 7b) and to the small hydraulic resistance of the filter cloth (Fig. 10a, solid line). Obviously, the filtration rate was high enough, then gradually decreased (Fig. 10b, dash line), while the filtrate volume rapidly increased (Fig. 10b, solid line).

For the time (II), the rates of H_{cake} and R_{cake} growth slow down due to the almost complete filling of the 1st type pores at the inlet of the filter cloth that led to porosity as low as 5% (Fig. 6c). As a result, the hydraulic resistance coefficient of the filter cloth increases sharply, and the filtration rate decreases considerably. The rate of increasing the filtrate volume slows down, as well.

For the time (III), the process is limited by the rate of the particles deposition on the filter surface, i.e. by the cake height. The rates of H_{cake} and R_{cake} growth are nearly constant. The particles cannot penetrate into the filter cloth, and quantities of R_F and the rate of the filtrate volume increase are practically constant.

It is worth to analyze in more details the accumulation of the particles on the filter surface. The dynamics of the cake's height growth is

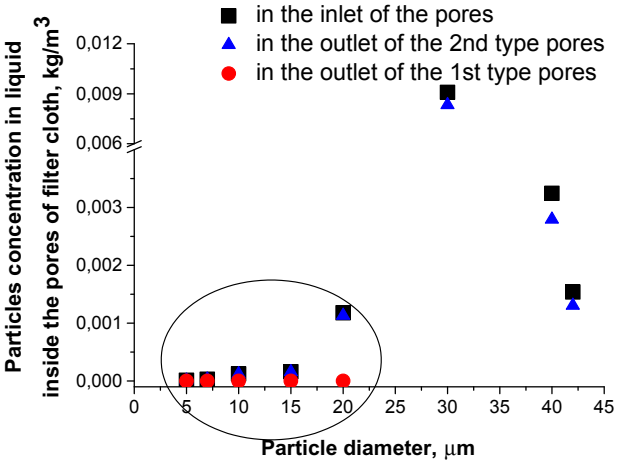

Fig. 8. Capturing the particles of different sizes inside the pores. Squares and circles – inlet and outlet concentration of particles 5–20 μm in size in the 1st type pores; Squares and triangles – inlet and outlet concentration of particles 5–42 μm in size in the 2nd type pores. $C^{in} = 1.7\ kg/m^3$, $d_1^0 = 20\ \mu m$, $d_{f\,1}^0 = 20\ \mu m$, $\varepsilon_1^0 = 0.3$, $d_2^0 = 42\ \mu m$, $d_{f\,2}^0 = 375\ \mu m$, $\varepsilon_2^0 = 0.008$, $t = 6\ s$.

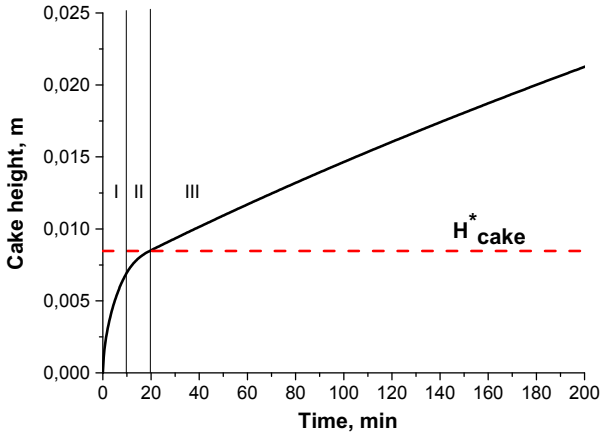

Fig. 9. Cake's height growth with time. Dotted line corresponds to H_{cake}^*. $C^{in} = 1.7\ kg/m^3$, $d_1^0 = 20\ \mu m$, $d_{f\,1}^0 = 20\ \mu m$, $\varepsilon_1^0 = 0.3$, $d_2^0 = 42\ \mu m$, $d_{f\,2}^0 = 375\ \mu m$, $\varepsilon_2^0 = 0.008$.

shown in Fig. 9. The cake is formed just in 7 s after the process beginning, and only the particles less than 20 μm in size can reach the inlet and outlet of the 2nd type pores (the oval area in Fig. 8). Starting from this moment, all the particles larger than 20 μm in size build-up on the surface to make the cake higher, while the particles smaller than 20 μm, depending on size, are either captured almost all in the 1st type pores or pass (85–99.6% of particles) through the filter cloth along the 2nd type pores to the bulk filtrate. During a period of ~ 20 min, the outlet concentrations change negligibly, within less than 0.02%. In 20 min, the cake's height grows to H_{cake}, see dashed line in Fig. 9; after that, the particles can no more penetrate into the filter but remain on the surface. This moment corresponds to the onset of the particles free clear oil production.

At the beginning of filtration, hydraulic resistance coefficient of the filter cloth increases sharply in time due to the quick accumulation of particles inside the filter space (Fig. 10a). Then it takes the constant value because no more particles penetrate into the filter. Hydraulic resistance coefficient of the cake R_{cake} rapidly increases at the beginning, as well. Then it increases more slowly because the filtration rate is decreasing (Fig. 10b, dash line).

4.2. Fitting experimental data by the model predictions

Details of the experimental procedure and obtained results have been mentioned above in Section 3. In Fig. 5 symbols indicate the experimental data relating to 3 consecutive cycles of filtration; lines are the results of simulation. It has been established that for adequate process simulation, it is critical to take into account the particle size distribution (Table 2) in the model. For example, in the 1st cycle of filtration fair agreement between the experimental data (square symbols) and model prediction (line A) is demonstrated in Fig. 5, while poor agreement exists if the weighted average particles diameter is assumed (dotted line). The weighted average particle diameter equal to 148 μm was determined from the actual particles size distribution (Table 1).

Rather good fitting the experimental points by calculated curves confirmed the validity of the accepted assumptions of the model set forth in subSections 2.1.1 and 2.1.2, as well as the values of the parameters ε_c, d_c and H_{cake}^* used. It should be mentioned that the best agreement obtained for the 1st cycle is mainly due to the fact that filtration on initially clean fabric occurred during this cycle. Experiments showed that complete discharge of the particles from the filter by means of blowing it with compressed air at 0.45 MPa was hardly possible. After each cycle, some of the particles retained inside the filter despite the blowing. Therefore, we have additionally assumed in the

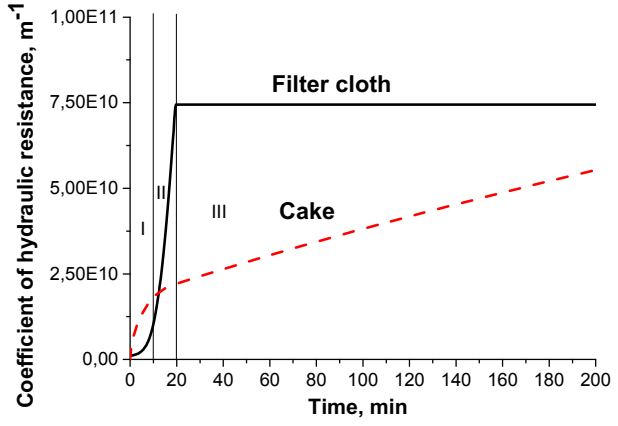

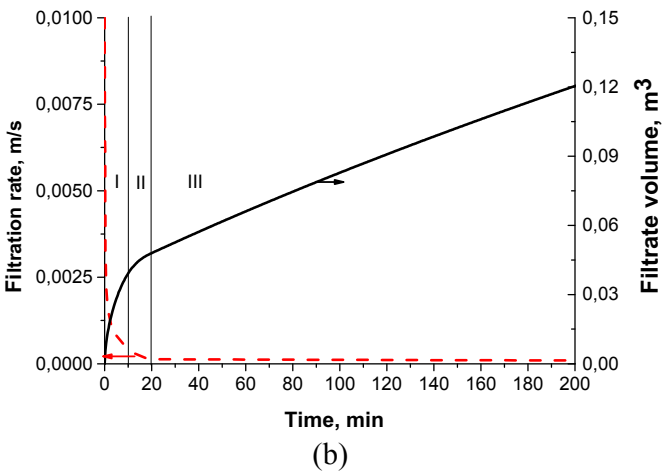

Fig. 10. Time variation: (a) hydraulic resistances of the filter cloth and of the cake; (b) filtration rate and volume of filtrate passed. $C^{in} = 1.7\ kg/m^3$, $d_1^0 = 20\ \mu m$, $d_{f\,1}^0 = 20\ \mu m$, $\varepsilon_1^0 = 0.3$, $d_2^0 = 42\ \mu m$, $d_{f\,2}^0 = 375\ \mu m$, $\varepsilon_2^0 = 0.008$.

Table 2
Parameters used for modeling the filtration process.

Parameter			Value	Dimension
T			80.0	°C
ΔP			0.25	mPa
S			0.06	m^2
L			0.0005	m
n			3.7	–
C^{in}			1.7	$kg{\cdot}m^{-3}$
ρ_{solid}			463.0	$kg{\cdot}m^{-3}$
ρ_{liquid}			855.0	$kg{\cdot}m^{-3}$
μ			0.02	Pa·s
G			40	kg
C^{iin}		d_p^i, μm	–	–
		5	$0.0000075{\cdot}C^{in}$	$kg{\cdot}m^{-3}$
		7	$0.000018{\cdot}C^{in}$	–//–
		10	$0.000072{\cdot}C^{in}$	–//–
		15	$0.000094{\cdot}C^{in}$	–//–
		20	$0.00069{\cdot}C^{in}$	–//–
		30	$0.0053{\cdot}C^{in}$	–//–
		40	$0.0019{\cdot}C^{in}$	–//–
		42	$0.0009{\cdot}C^{in}$	–//–
		50	$0.009{\cdot}C^{in}$	–//–
		75	$0.019{\cdot}C^{in}$	–//–
		125	$0.47{\cdot}C^{in}$	–//–
		175	$0.471{\cdot}C^{in}$	–//–
		210	$0.022{\cdot}C^{in}$	–//–
u^0			0.01	$m{\cdot}s^{-1}$
H^*_{cake}			0.00847	m
Filter cloth	1st type of pores	d_1^0	20.0	μm
		$d^0_{f\,1}$	20.0	μm
		ε_1^0	0.3	–
	2nd type of pores	d_2^0	42.0	μm
		$d^0_{f\,2}$	375.0	μm
		ε_2^0	0.008	
	K_F		48.0	–
Cake	d_c		20.0	μm
	ε_c		0.4	–
	K_c		150.0	–
Δt			1	s
J			15	–

Table 3
Influence of parameters on the process performance.

I – Effect of the particles concentration		C^{in}, kg/m^3		
Time elapsed, min		2.4	1.7	1
25	t_n, min	102.9	100.5	56.15
200	t_n, min	146.6	133.5	120.0
	$t_{H^*_{cake}}$, min	13.7	19.5	32.7
200	$\chi(t)$, %	99.995	99.996	99.997
II – Effect of the porosity of the 1st type		$\varepsilon_1^0(\varepsilon_2^0 = 0.008)$		
Time elapsed, min		0.2	0.3	0.4
25	t_n, min	270.0	100.5	33.57
200	t_n, min	733.8	133.5	94.1
	$t_{H^*_{cake}}$, min	> 200	19.5	12.0
200	$\chi(t)$, %	99.988	99.996	99.997
III – Effect of the porosity of the 2nd type		$\varepsilon_2^0(\varepsilon_1^0 = 0.3)$		
Time elapsed, min		0.006	0.008	0.01
25	t_n, min	109.2	100.5	92.9
200	t_n, min	140.2	133.5	127.9
	$t_{H^*_{cake}}$, min	20.0	19.5	19.0
200	$\chi(t)$, %	99.9958	99.9960	99.9961
IV – Effect of the fiber size		$d^0_{f\,1}$, μm ($d^0_{f\,2}$ = 375 μm)		
Time elapsed, min		10	20	30
25	t_n, min	281.6	100.5	33.4
200	t_n, min	297.5	133.5	94.0
	$t_{H^*_{cake}}$, min	> 200	19.5	12.7
200	$\chi(t)$, %	99.987	99.996	99.998
V – Effect of the thread size		$d^0_{f\,2}$, μm ($d^0_{f\,1}$ = 20 μm)		
Time elapsed, min		300	375	450
25	t_n, min	103.6	100.5	99.1
200	t_n, min	135.9	133.5	132.5
	$t_{H^*_{cake}}$, min	22.6	19.5	19.3
200	$\chi(t)$, %	99.9962	99.996	99.9958
VI – Effect of the 1st type pores size		d_1^0, μm (d_2^0 = 42 μm)		
Time elapsed, min		10	20	30
25	t_n, min	33.5	100.5	202.6
200	t_n, min	94.1	133.5	222.7
	$t_{H^*_{cake}}$, min	15.6	19.5	202.0
200	$\chi(t)$, %	99.997	99.996	99.989
VII – Effect of the 2nd type pores size		d_2^0, μm (d_1^0 = 20 μm)		
Time elapsed, min		30	42	50
25	t_n, min	111.0	100.5	98.4
200	t_n, min	151.0	133.5	132.8
	$t_{H^*_{cake}}$, min	21.0	19.5	19.0
200	$\chi(t)$, %	99.997	99.996	99.985

model that 2.5% of the captured particles remain inside the filter after the 1st filter discharge, 5% – after the 2nd discharge. This led to a stepwise increase of t_n value observed after each cycle. Under these assumptions, we obtained satisfactory agreement between theoretical predictions and experimental points for each of three filtration cycles followed by two filter discharges, see Fig. 5.

4.3. Influence of the parameters on the filtration process

The filtering time necessary for complete removal of the solids from a certain batch of suspension t_n and the degree of suspension purification $\chi(t)$, indicate the quality of the filtration process. To achieve high process efficiency, it is necessary:

1) Minimum t_n that is equivalent to the maximum amount of the filtrate produced per a fixed process time;
2) Maximum degree of the suspension purification from the catalyst.

Porous structure of the filter and concentration of the particles in suspension are the parameters that have the greatest impact on the filtration process. The effect of these parameters on the process indicators t_n and $\chi(t)$ was investigated using the filtration model given in Section 2 and specifications listed in Table 2; originally clean filter cloth was supposed. Values of t_n were determined for two moments of the time elapsed since the filtration onset: $t = 25$ min, i.e. at the beginning of the process; and $t = 200$ min, i.e. close to the end of the process. The degree of suspension purification during the time interval t was estimated as follows:

$$\chi(t) = \frac{m^{in}(t) - \int_0^t m^{out} dt}{m^{in}(t)}, \quad t = 200 \text{ min} \tag{24}$$

The simulation results are summarized in Table 3.

4.3.1. Influence of concentration of particles C^{in}

Increasing the concentration of particles of all sizes in the flow upstream the filter cloth from 1 to 2.4 kg/m^3 leads to an increase in t_n by factor of 1.8 at $t = 25$ min and by factor of 1.2 at $t = 200$ min, see Table 3, Part I. An increase in the concentration of particles also contributes to an increase in the hydraulic resistance coefficient of the filter cloth, and consequently to a faster growth of the alluvial layer: by the end of the cycle, the time $t_{H^*_{cake}}$ necessary for the formation of a cake with a height H^*_{cake} decreases approximately in inverse proportion to the concentration of the particles. With increasing C^{in}, the filtrate volume and purification degree slightly decrease.

4.3.2. Influence of porosity

The total porous structure of the filter cloth is formed from the pores of the 1st and 2nd types, their porosities are ε_1^0 and ε_2^0, respectively. Porosity ε_1^0 has a great impact upon parameters during the whole cycle (Table 3, Part II). If the filter porosity ε_1^0 is large, then t_n value is low because the pores are not plugged yet, and the hydraulic resistance of the filter is small. With a decrease in ε_1^0, an increase in R_F occurs. The total filtering efficiency η_1^i drops sharply, which reduces the filtration rate and the volume filtrated. A two-fold decrease in ε_1^0 from 0.4 to 0.2 results in 8-fold increase in t_n and 16-fold increase in $t_{H^*_{cake}}$. The efficiency of the fat purification $\chi(t)$ is negligibly changing under ε_1^0 variation.

As the porosity caused by the 2nd type pores ε_2^0 is relatively small, their effect on the process parameters is much less than that of the 1st type pores during the whole cycle (Table 3, Part III). With increasing ε_2^0 from 0.006 to 0.01, the filtration time t_n reduced by 10–17% only, while the efficiency of filtration $\chi(t)$ and the time of the cake growth $t_{H^*_{cake}}$ did not change.

4.3.3. Influence of fiber diameter

In the filtering fabric, the pores of the 1st type are formed by the separate fibers of diameter $d^0_{f\,1}$ and create porosity ε_1^0, the pores of the 2nd type are formed by the groups of fibers twisted into the thread (or filament) of diameter $d^0_{f\,2}$ and create porosity ε_2^0.

Fiber diameter strongly affects the process parameters (Table 3, Part IV). The smaller fiber diameter, the larger specific area of fiber edges; that leads to a greater opportunity to trap the particles and increases the total capturing efficiency η_1^i. However, if $d^0_{f\,1}$ decreases from 30 to 10 μm, the t_n value significantly grows by factor of 8.4 at $t = 25$ min and by factor of 3.2 at $t = 200$ min. The reason is that at $d^0_{f\,1} = 10$ μm hydraulic resistance coefficient R_F increases by two orders of magnitude, causing considerable decrease in the filtration rate. The cake's height is less than H^*_{cake} for the whole process time. As a result, the purification degree $\chi(t)$ is slightly reduced, although η_1^i increased.

A decrease in the thread diameter $d^0_{f\,2}$ from 450 to 300 μm has minor impact on the process parameters (Table 3, Part V), because of a small proportion of the 2nd type pores in the filter cloth. Time t_n grows a little, and $\chi(t)$ slightly increases due to an increase in η_2^i.

4.3.4. Influence of pore diameter

The influence of the pore size of each type is similar to that of the diameters of the fibers, respectively (Section 4.3.2). As to the 1st type pores (Table 3, Part VI), the smaller pore size d_1^0, the lower t_n because the particles larger thand_1^0in diameter deposit on the filter surface rather than penetrate into the filter medium; the hydraulic resistance of the filter cloth remains small, and it takes less time to reach H^*_{cake}. Smaller pores provide higher purification degree due to both lower$t_{H^*_{cake}}$, and higher η_1^i.

Variating the 2nd type pores diameter has little effect on the parameters. A decrease in$d_2^0$from 50 to 30 μm results in a mere 12–13% increase in t_n due to the improved capturing efficiency (Table 3, Part VII). As to the large pores, η_2^i decreases, t_n and $t_{H^*_{cake}}$ are shorter, and larger particles can enter the filter. So, at least at the initial filtering period, particles smaller than 50 μm can penetrate into the pores with $d_2^0 = 50$ μm. For this reason, the larger pores provide lower purification degree.

Thus, the improved efficiency of the process, namely, a short filtration time t_n and a high degree of purification $\chi(t)$ is favored by:

- Decreasing the concentration of particles in the suspension;
- Increasing the porosity generated by the 1st and 2nd types of the pores;
- Increasing the thread diameter;
- Decreasing of the first type pores diameter.

An increase in the diameter of fiber or second type pores makes t_n shorter; however, the purification degree decreased as well. In the range of parameters under consideration, no more than 15% of particles, depending on their size, are captured in the second type pores. Therefore, it is reasonable to select the filter cloth with finer threads and smaller pores to improve the purification degree.

5. Conclusions

An unsteady-state mathematical model with distributed parameters is developed which describes the filtration of the catalyst suspension in hydrogenated oil through a porous woven cloth. The model takes into account the main physical features of the process, such as porous structure of the filter, percolation of particles through the filter pores, accumulation of particles inside the filter pores, and a cake growth. With a known particle size distribution, the model allows estimating the time necessary for the filtration of a fixed amount of suspension and the degree of suspension purification. The impact on the process efficiency by filter porosity, fiber and pore diameters, and concentration of particles in the suspension is analyzed. Simulation results show that polydisperse particles can both percolate through the filter cloth and accumulate inside it as well as on its surface. High efficiency is favored by a proper selection of the filter media having sufficient porosity, large fiber and thread diameters, and small diameter of the pores formed by the fibers.

The model prediction was verified by the cyclic mode filtration experiments obtained on a lab-scale setup. The model describes the dynamic regimes for 3 cycles with acceptable accuracy; this allow us to determine the time required for a complete filtration of a definite particles batch from a given liquid volume.

With the model first time proposed in this paper, it is possible to predict the performance of industrial filters and to select the filtering material with the proper specifications for efficient separation of the catalyst from hydrogenated oil products after slurry reactors.

Acknowledgement

The authors are grateful to Dr. E.I. Smirnov for his assistance in experimental work and for useful discussions in preparing the manuscript.

This work was conducted within the framework of the budget project for Boreskov Institute of Catalysis.

Appendix A

Filter cloth porosity. The porosity formed by the second type pores, ε_2^0, equal to 0.008 was determined based on the calculation of the area of four pores within the square with 833 μm side (Fig. 2).

The porosity formed by the first type pores, ε_1^0, was estimated based on the experimental results on the filtration of pure hydrogenated fat (expression (14)) at the other known parameters. In filtration of pure hydrogenated fat, the cake height $H_{cake} = 0$. The porosity was chosen so as to provide coincidence of the filtration rate, $\frac{1}{S}\left(\frac{dV_{Filtrate}}{dt}\right)$, and the rate determined experimentally from formula (22) under G = 40 kg. The result was $\varepsilon_1^0 = 0.03$.

Coefficient K_F in formula (14), which depends only on the geometry of channels in the porous structure, was taken equal to 48 similar to the case of a liquid flow through long transversal interstices.

Cake sizes. The pore diameter in the cake layer, d_c, was estimated as the arithmetic average diameter of two circles inscribed into a three-particle ensemble. While the particles 100–200 μm in diameter occupy more than 94.1 wt% of the total particles (Table 1), the ones with 100 and 200 μm diameters were chosen as circles of the first and second ensembles, respectively. The pore diameter in the cake was estimated to be 20 μm.

The porosity of the layer comprising particles with different sizes can vary between 0.27 and 0.45 [28]. While the particles 100–200 μm in diameter are more than 94 wt% of the total number of particles

(Table 1) and majority of these particles are approximately identical in size (Fig. 3), the cake porosity, ε_c, was taken equal to 0.4.

Coefficient K_c in formula (14), which depends only on the geometry of channels in the porous structure, was taken equal to 150 similar to the case of a liquid flow through a bed of spherical particles.

Height of cake, H^*_{cake}, was estimated based on the experimental results. It was shown that the catalyst particles were not removed completely from the filtrate during the early 20 min when the particles can penetrate inside the filter cloth. Since 20 min elapsed, one can consider the filtrate free of the particles. Therefore, H^*_{cake} was estimated at the average filtration rate between the initial moment and in 20 min and during the filtration time equal to 20 min.

Concentration of all particles in the flow upstream the filter cloth, C^{in}, was calculated based on the experimental conditions: 40 g of solid material was added to 20 kg of the oil mixture. When the density $\rho_{liquid} = 855\ kg/m^3$, then $C^{in} = 1.7\ kg/m^3$. Since filtration of the first 20 kg portion of the suspension took ca. 50 min, and these were intervals for adding the catalyst, the obtained magnitude C^{in} was accepted constant.

Concentration of the particles of *i-th* size in the flow upstream the filter cloth, C^{iin}, was calculated based on the total concentration C^{in}, the known weight percentage of the particles (Table 1) and the results of additional experimental studies of the size distribution of particles in the post-filtered aqueous suspension. Particles larger than 42 μm in diameter were not observed in the suspension.

References

[1] E. Łodyga-Chruścińska, A. Sykuła-Zając, D. Olejnik, Determination of nickel in Polish brands of margarines, Food Additives Contaminants: Part B 5 (2012) 251–254, https://doi.org/10.1080/19393210.2012.702287.

[2] Codex Alimentarius Commission, Doc. no. CF/11 INF/1. Joint FAO/WHO food standards programme, Working document for information and use in discussions related to contaminants and toxins in the GSCTFF, 2017.

[3] L. Dohnalova, P. Bucek, P. Vobornik, V. Dohnal, Determination of nickel in hydrogenated fats and selected chocolate bars in Czech Republic, Food Chem. 217 (2017) 456–460, https://doi.org/10.1016/j.foodchem.2016.08.066.

[4] M.B. Fernandez, F. John, M. Sanchez, G.M. Tonetto, D.E. Damiani, Hydrogenation of sunflower oil over different palladium supported catalysts: activity and selectivity, Chem. Eng. J. 155 (2009) 941–949, https://doi.org/10.1016/j.cej.2009.09.037.

[5] N. Numwong, A. Luengnaruemitchai, N. Chollacoop, Y. Yoshimura, Effect of metal type on partial hydrogenation of rapeseed oil-derived FAME, J. Am. Oil Chem. Soc. 90 (2013) 1431–1438.

[6] R.M. Abdullina, I.N. Voropaev, A.V. Romanenko, V.A. Chumachenko, A.S. Noskov, A.S. Mashnin, Partial hydrogenation of sunflower oil: influence of the process conditions on the physicochemical properties of the products, Russ. J. Appl. Chem. 85 (8) (2012) 1204–1211.

[7] C. Tien, R. Bai, An assessment of the conventional cake filtration theory, Chem. Eng. Sci. 58 (2003) 1323–1336.

[8] C. Tien, S.K. Teoh, R.B.H. Tan, Cake filtration analysis – the effect of the relationship between the pore liquid pressure and the cake compressive stress, Chem. Eng. Sci. 56 (2001) 5361–5369.

[9] K. Stamatakis, C. Tien, Cake formation and growth in cake filtration, Chem. Eng. Sci. 46 (1991) 1917–1933.

[10] G.G. Chase, M.S. Willis, Compressive cake filtration, Chem. Eng. Sci. 47 (1992) 1373–1381.

[11] M.R. Mackley, N.E. Sherman, Cake filtration mechanisms in steady and unsteady flows, J. Membr. Sci. 77 (1993) 113–121, https://doi.org/10.1016/0376-7388(93)85239-S.

[12] R. Wakeman, The influence of particle properties on filtration, Separ. Purif. Tech. 58 (2007) 234–241.

[13] T.h. Neesse, J. Dueck, E. Djatchenko, Simulation of the filter cake porosity in solid/liquid separation, Powder Tech. 193 (2009) 332–336.

[14] A.S. Kim, E.M.V. Hoek, Cake structure in dead-end membrane filtration: Monte Carlo simulations, Env. Eng. Sci. 19 (2004) 373–386, https://doi.org/10.1089/109287502320963373.

[15] J.C.-T. Lin, T.-C. Hsiao, S.-S. Hsiau, D.-R. Chen, Y.-K. Chen, S.-H. Huang, C.-C. Chen, M.-B. Chang, Effects of temperature, dust concentration, and filtration superficial velocity on the loading behavior and dust cakes of ceramic candle filters during hot gas filtration, Sep. Purif. Technol. 198 (2018) 146–154, https://doi.org/10.1016/j.seppur.2017.06.014.seppur.2017.06.014.

[16] S. Osterroth, C. Preston, B. Markicevic, O. Iliev, M. Hurwitz, The permeability prediction of beds of poly-disperse spheres with applicability to the cake filtration, Sep. Purif. Technol. 165 (2016) 114–122, https://doi.org/10.1016/j.seppur.2016.03.046.

[17] P.M. Heertjes, P.L. Zuideveld, Clarification of liquids using filter aids, part ii. Depth filtration, Powder Technol. 19 (1978) 31–43.

[18] C.R. Ison, K.J. Ives, Removal mechanisms in deep bed filtration, Chem. Eng. Sci. 24 (1969) 717–729.

[19] G. Saracco, C. Badini, V. Specchia, Catalytic traps for diesel particulate control, Chem. Eng. Sci. 54 (1999) 3035–3041.

[20] S.H. Oh, J.S. MacDonald, G.L. Vaneman, L.L. Hegedus, Mathematical modeling of fibrous filters for diesel particulates – theory and experiment, SAE Technical Paper Series 810113 (1981) 112.

[21] R.C. Brown, D. Wake, Air filtration by interception – theory and experiment, J. Aerosol Sci. 22 (2) (1991) 181–186.

[22] N. Tufenkji, M. Elimelech, Correlation equation for predicting single-collector efficiency in physicochemical filtration in saturated porous media, Environ. Sci. Technol. 38 (2004) 529–536.

[23] T.L. Pavlova, N.V. Vernikovskaya, N.A. Chumakova, A.S. Noskov, Analysis of thermal processes in catalytic particulate filters, Combust. Expl. Shock Waves 40 (3) (2004) 263–269.

[24] T.L. Pavlova, N.V. Vernikovskaya, N.A. Chumakova, A.S. Noskov, Regeneration of a catalytic filter in the presence of highly flammable hydrocarbons in soot, Combust. Expl. Shock Waves 42 (4) (2006) 396–402.

[25] N.V. Vernikovskaya T.L. Pavlova N.A. Chumakova A.S. Noskov, Mathematical modelling of filtration and catalytic oxidation of diesel particulates in filter porous media, in: J.C. Cortés L. Jódar R. Villanueva Mathematical Modeling in Social Sciences and Engineering, Nova Sciences Publishers, Inc. Hauppauge, NY, 2014, pp. 27–40 (ISBN: 978-1-63117-335-6).

[26] N.V. Vernikovskaya, T.L. Pavlova, V.V. Mokrinskii, D.Yu. Murzin, N.A. Chumakova, A.S. Noskov, Soot particulates abatement in diesel engine exhaust by catalytic oxidation followed their trapping in filters, Chem. Eng. J. 269 (2015) 416–424, https://doi.org/10.1016/j.cej.2015.01.129.

[27] V.A. Zhuzhikov, Filtration, Theory and Practice of Suspensions Separation, Khimiya, Moscow, 1980 (in Russian).

[28] M.E. Aerov, M.O. Todes, D.A. Narinskii, Apparatuses with Fixed Granular Beds, Khimiya, Leningrad, Russia, 1979 (in Russian).

[29] E.A. Novikov, Numerical methods for solution of differential equations in chemical kinetics, in: V.I. Bykov (Ed.), Mathematical methods in chemical kinetics, Nauka, Novosibirsk, 1990, pp. 53–68 (in Russian).

[30] N.V. Vernikovskaya, An equation-oriented approach to modeling heterogeneous catalytic reactors, Chem. Eng. J. 329 (2017) 15–24, https://doi.org/10.1016/j.cej.2017.05.095.